

RESEARCH

Open Access



# Human pancreatic islet-derived stromal cells reveal combined features of mesenchymal stromal cells and pancreatic stellate cells

Nour Ebrahim<sup>1,6</sup>, Nikolay Kondratyev<sup>2</sup>, Alexander Artyuhov<sup>1,3</sup>, Alexei Timofeev<sup>1</sup>, Nadya Gurskaya<sup>1</sup>, Alexey Andrianov<sup>4</sup>, Roman Izrailov<sup>4</sup>, Egor Volchkov<sup>3,7</sup>, Tatyana Dyuzheva<sup>8</sup>, Elena Kopantseva<sup>3</sup>, Ekaterina Kiseleva<sup>5</sup>, Vera Golimbet<sup>2</sup> and Erdem Dashinimaev<sup>1,3,6,9\*</sup> 

## Abstract

**Background** Mesenchymal stromal cells (MSCs) are recognized for their potential in regenerative medicine, attributed to their multipotent differentiation capabilities and immunomodulatory properties. Despite this potential, the classification and detailed characterization of MSCs, especially those derived from specific tissues like the pancreas, remains challenging leading to a proliferation of terminology in the literature. This study aims to address these challenges by providing a thorough characterization of human pancreatic islets-derived mesenchymal stromal cells (hPD-MSCs).

**Methods** hPD-MSCs were isolated from donor islets using enzymatic digestion, immortalized through lentiviral transduction of human telomerase reverse transcriptase (hTERT). Cells were characterized by immunostaining, flow cytometry and multilineage differentiation potential into adipogenic and osteogenic lineages. Further a transcriptomic analysis was done to compare the gene expression profiles of hPD-MSCs with other mesenchymal cells.

**Results** We show that hPD-MSCs express the classical MSC features, including morphological characteristics, surface markers expression (CD90, CD73, CD105, CD44, and CD106) and the ability to differentiate into both adipogenic and osteogenic lineages. Furthermore, transcriptomic analysis revealed distinct gene expression profiles, showing notable similarities between hPD-MSCs and pancreatic stellate cells (PSCs). The study also identified specific genes that distinguish hPD-MSCs from MSCs of other origins, including genes associated with pancreatic function (e.g., ISL1) and neural development (e.g., NPTX1, ZNF804A). A novel gene with an unknown function (ENSG00000286190) was also discovered.

**Conclusions** This study enhances the understanding of hPD-MSCs, demonstrating their unique characteristics and potential applications in therapeutic strategies. The identification of specific gene expression profiles differentiates hPD-MSCs from other mesenchymal cells and opens new avenues for research into their role in pancreatic function and neural development.

**Keywords** Pancreatic mesenchymal stromal cells, Pancreatic stellate cells, Transcriptome analysis, Pancreatic islets, Pancreas

\*Correspondence:

Erdem Dashinimaev  
dashinimaev@gmail.com

Full list of author information is available at the end of the article



© The Author(s) 2024. **Open Access** This article is licensed under a Creative Commons Attribution-NonCommercial-NoDerivatives 4.0 International License, which permits any non-commercial use, sharing, distribution and reproduction in any medium or format, as long as you give appropriate credit to the original author(s) and the source, provide a link to the Creative Commons licence, and indicate if you modified the licensed material. You do not have permission under this licence to share adapted material derived from this article or parts of it. The images or other third party material in this article are included in the article's Creative Commons licence, unless indicated otherwise in a credit line to the material. If material is not included in the article's Creative Commons licence and your intended use is not permitted by statutory regulation or exceeds the permitted use, you will need to obtain permission directly from the copyright holder. To view a copy of this licence, visit <http://creativecommons.org/licenses/by-nc-nd/4.0/>.

## Introduction

Recent progress in stem cell biology and regenerative medicine has given rise to translational research aimed at repairing damaged tissues and restoring their proper cellular functions. MSCs stand out as an important candidate in the field of cellular therapy, having undergone extensive investigation and clinical trials. The therapeutic benefits of MSCs lie in their ease of extraction, ability to differentiate into various cell types, minimal immune response, and, most significantly, the substances they release, which have been demonstrated to mitigate damaged tissues [1].

Despite the prospective advantages of MSCs, practical constraints arise due to the inherent challenges associated with the isolation process and heterogeneity arising from diverse donor characteristics [2]. While all MSCs share basic characteristics, studies have shown variances in genotype and phenotype expression profiles among MSCs of different sources including expression of certain surface markers, differentiation capacities, and immunomodulatory properties [3, 4]. These differences extend to the physiological functions of MSCs and their therapeutic potential in the treatment of diverse diseases.

This highlights the significance of a nuanced characterization of MSCs for effective utilization in clinical applications, considering logistical, practical, and *in vivo* attributes. MSCs were initially isolated from mononuclear cells derived from bone marrow (BM-MSCs); nevertheless, recent evidence suggests that MSCs are present in almost all human tissues [5]. Notably, the pancreas harbors distinct subpopulations of MSCs, with evidence indicating that these cells can be derived from exocrine tissue (acinar and ductal epithelial cells) [6–8], or islets [9, 10]. The precise etiology of these cells remains ambiguous, potentially arising from epithelial-mesenchymal transition or the homing of mesenchymal stromal cells from the bone marrow [11, 12]. Mesenchymal stromal cells derived from the pancreatic islets, denoted as Pancreas-Derived MSCs (PD-MSCs), exhibit hallmark characteristics typical of MSCs. These characteristics encompass morphological features, surface cell marker expression, and differentiation potential [8]. Moreover, PD-MSCs have been demonstrated to give rise to pancreatic endocrine progenitors as evidenced by the expression of endocrine progenitor markers upon *in vitro* expansion [10, 13].

Despite the potentially pivotal role that PD-MSCs could play in the treatment of pancreatic diseases, they remain understudied in the existing literature. Hence, in this study, we present a comprehensive analysis of PD-MSCs, with a particular focus on their transcriptomic profile. Our findings indicate that stromal cells derived from the pancreas demonstrate characteristics

reminiscent of stem cells, closely resembling stellate cells. Additionally, PD-MSCs express markers associated with both pancreatic and neuronal identities. This unique combination of features suggests advantages in utilizing pancreatic stromal cells for the treatment of pancreatic diseases, distinguishing them from other types of stromal cells.

## Materials and methods

### Isolation and culture of hPD-MSCs and control MSCs lines

The human pancreatic tail specimens were taken by incision biopsy after distal pancreatectomy or laparoscopic pancreatoduodenectomy in five patients (age  $\geq 45$  yr, M:F = 3:2) diagnosed with pancreatic cancer. This part of the study was conducted in accordance with the Declaration of Helsinki and the legislation of the Russian Federation on human health protection. The use of biopsied tissue for scientific purposes was approved by the Ethical Board at the Loginov Moscow Clinical Scientific Center (Board Record #1/2020 of February 3, 2020). All patients provided written informed consent for biospecimen donation and signed a special agreement for participation in scientific research. Within 2 h, the material was transported to the lab in an ice-cold  $\alpha$  Minimum Essential Medium (Paneco, Russia) with 15% fetal bovine serum (FBS) (Biosera, France), 2% penicillin/streptomycin (Gibco, USA), and 300 KIU/ml aprotinin (Sigma-Aldrich, USA). The material was then processed according to a composite of established protocols [14–16]. Briefly, the specimen was dissected with scissors into smaller fragments and rinsed with Hank's Balanced Salt Solution (Paneco, Russia), then it was incubated in collagenase solution (200 IU/ml) (Paneco, Russia) for 30 min at 37 °C with continuous agitation. The digested material was centrifuged and the supernatant was discarded, the resulting pellet was gently overlaid onto 10 ml of Ficoll 1.077 (Paneco, Russia) followed by centrifugation for 18 min at 900 g. The supernatant contained the islets while the pellet was rich with pancreatic exocrine cells. The supernatant was sieved through a 70  $\mu$ m strainer for islet collection. Collected islets were transferred to an appropriate Petri dish and cultured in an initial growth medium (Dulbecco's Modified Eagle Medium (DMEM) (Paneco, Russia), 10% FBS, 1% GlutaMAX (Corning, USA), 1% sodium pyruvate (Gibco, USA), 1% penicillin/streptomycin). The medium was changed every three days until cells attained 80–90% confluency. Bone marrow-derived MSCs (BM-MSCs) and adipose tissue-derived MSCs (AT-MSCs) were obtained from the cell collection of the N.K. Koltsov Institute of Developmental Biology (Russian Academy of Science, Moscow, Russia), and were cultured in DMEM, 10% FBS, 1% GlutaMAX, 1% penicillin/streptomycin, 1% Insulin-Transferrin-Selenium (Gibco, USA).

human immortalized dermal fibroblast cell culture was kindly provided by Dr. Yegorov E.E. (Engelhardt Institute of Molecular Biology, RAS) and was cultured in the same condition as PD-MSCs.

#### Lentiviral production

Lentiviral plasmids for packaging—pLP1, pLP2, and pVSVG (Invitrogen, ViraPower™ Lentiviral Expression Systems) – were employed to assemble lentiviral particles in the HEK293TN cell line. A total of  $2 \times 10^6$  HEK 293TN cells were seeded into pre-prepared 6 cm Petri dishes coated with a 1% gelatin solution, using 4.5 ml of DMEM supplemented with 10% FBS and 1% antibiotic, sodium pyruvate, and glutamine one day before transfection. On the day of transfection, a reaction mixture comprising packaging plasmids and the vector with gRNA (equimolar mix) was prepared in a serum-free OptiMEM medium. Transfection was conducted using Polyethylenimine as a transfection agent in a low-serum medium (DMEM supplemented with 2% FBS, 0.2% antibiotic, 1% sodium pyruvate, and 1% glutamine). After 24 h, the medium was replaced with a fresh complete growth medium (DMEM supplemented with 10% FBS, 1% antibiotic, sodium pyruvate, and glutamine). The reaction mixture was incubated for 27 h to allow assembling of viral particles. Following assembly, the virus supernatant was harvested and filtered through a 0.45  $\mu\text{m}$  filter.

#### Immortalization of hPD-MSCs with htert

hPD-MSCs were immortalized by stable expression of human Telomerase Reverse Transcriptase cDNA (hTERT). The lentiviral plasmid construct encoding hTERT was described previously [17]. The hTERT fragment was delivered by lentiviral transduction with 5  $\mu\text{g}/\text{ml}$  Polybrene (Serva, Germany). Positive selection, employing puromycin (Sigma-Aldrich, USA) was executed over a two-passage duration one week post-transduction. The selected cell populations propagated in vitro in parallel with non-transduced cells as controls.

#### Immunocytochemical staining

For immunocytochemical staining, the cells were washed with Dulbecco's Phosphate-Buffered Saline solution (DPBS) and were fixated for 15 min in 4% paraformaldehyde at room temperature. Following this fixation, the cultures underwent another round of washing with DPBS before incubation with primary antibodies (Supplementary Table S1) in a blocking solution (PBS with 10% FBS, 0.1% Triton X-100, and 0.01% Tween-20) overnight at  $+4^\circ\text{C}$ . Subsequently, the cellular cultures were washed three times with DPBS (5 min each at room temperature) and incubated with secondary antibodies (Alexa Fluor 546 goat anti-mouse IgG (Invitrogen, #A11030) or Alexa

Fluor 488 donkey anti-rabbit IgG (Invitrogen, #A32790) diluted 1:1000 in the blocking solution for 1 h at  $37^\circ\text{C}$ . The cell nuclei were contrasted with DAPI (1 mg/ml in PBS). Imaging was conducted using an EVOS FL AUTO (Life Technologies) fluorescence microscope.

#### Flow cytometry

Cell surface markers were studied using flow cytometry. Briefly, around  $2 \times 10^6$  cells were harvested using trypsinization followed by fixation using 4% paraformaldehyde (Sigma-Aldrich, USA) for 15 min at room temperature. Cells were washed with DPBS and incubated with specific monoclonal antibodies (Supplementary Table S1) in blocking solution (PBS with 10% FBS, 0.1% Triton X-100, and 0.01% Tween-20) for 1 h at  $37^\circ\text{C}$  with constant shaking, followed by three washes with DPBS to remove unbound antibodies and subsequently analyzed using Flow Cytometer (BioRad S3e, BioRad, USA) compared to control samples. The resulting data were acquired and analyzed through FlowJo software 10.8.1 (Becton, USA) and are presented as the average of three independent repeats at least with standard deviation.

#### Adipogenic and osteogenic differentiation

Immortalized PD-MSCs were differentiated into osteoblasts and adipocytes. For adipogenic differentiation, cells were seeded in a 12-well plate using a standard culture medium. The following day, the medium was changed to DMEM supplemented with 10% FBS, 1% GlutaMAX, 1  $\mu\text{M}$  Dexamethasone (Sigma-Aldrich, USA), and 10  $\mu\text{M}$  insulin (Gibco, USA). The medium was changed periodically every 2–3 days for 15–20 days, subsequently, cells were fixed using 4% paraformaldehyde and stained with Oil Red O (Sigma-Aldrich, USA) and 0.4% Trypan blue (Bio-Rad, USA). Briefly, cells were rinsed with 60% isopropanol and incubated for 10 min in Oil Red O dissolved in 98% isopropanol. The dye was subsequently removed and cells were washed with 60% isopropanol followed by DPBS (Paneco, Russia).

For osteogenic differentiation, cells were seeded in a 12-well plate using a standard culture medium, to be changed the next day to DMEM supplemented with 10% FBS, 1% GlutaMAX, 0.01  $\mu\text{M}$  dihydroxy vitamin D3 (Sigma-Aldrich, USA), 50  $\mu\text{M}$  ascorbate-2-phosphate (Sigma-Aldrich, USA), 10 mM  $\beta$ -Glycerophosphate (Sigma-Aldrich, USA). After 2–3 weeks, cells were fixed with 4% paraformaldehyde and stained with Alizarin Red S (Sigma-Aldrich, USA) and 0.4% trypan blue. Briefly, cells were incubated for 2 min with the dye dissolved in distilled water with a pH range of 6.3–6.5. Subsequently, cells were washed with distilled water followed by a second wash with 1 mM HCL in 95% ethanol and examined under light microscopy.

### Quantitative real-time polymerase chain reaction (RT-qPCR)

One million cells were collected via centrifugation and total RNA was extracted using RNeasy Mini Kit (Qiagen, Germany), following the manufacturer's instructions. The quality and quantity of RNA samples were assessed with a NanoPhotometer P360 (Implen, Germany). One microgram of total RNA was utilized to synthesize cDNA. Firstly, genomic DNA was eliminated using the RNase-free DNase Set (Qiagen, Germany) following the manufacturer's instructions. First-strand cDNA was obtained using a Reverse transcriptase MMLV kit (Evrogen, Russia), following the manufacturer's protocol with 1.5  $\mu$ M of Oligo (dT)<sub>15</sub>/Random (dN)<sub>10</sub> mixture (1:1) with 100 e.u. of MMLV per reaction. RT-qPCR was performed using the 7500 Real-Time PCR System (Applied Biosystems, USA). The temperature profile comprised three steps: an initial 10-min incubation at 95 °C, followed by 40 cycles of denaturation at 95 °C for 15 s, and annealing/extension at 60 °C for 1 min. Subsequently, a melt curve analysis was performed within the temperature range of 60 °C to 95 °C. The reaction mixes were prepared using HS-SYBR (Evrogen, Russia).

Primers for RT-qPCR analysis were designed using Primer Blast (Supplementary Table S2), and calculations were executed using the  $-\Delta\Delta C_T$  method. We used the geNorm algorithm to choose *EMC7*, *PSMB4*, and *RPL27* for normalization from the list of 6 candidates (*ACTB*, *C1orf43*, *EMC7*, *GAPDH*, *PSMB4*, *RPL27*). Each target gene was subjected to three independent biological and technical replicates. The  $C_T$  data from the three independent repeats were averaged to determine the mean  $C_T$  values and  $C_T$  standard deviation. Subsequently, an analysis of variance (ANOVA) was employed to assess the statistical significance of the observed differences.

### Transcriptome analysis

To prepare samples for transcriptome analysis, mRNA was isolated as described in the RT-qPCR section and processed with a DNase I (Thermo Fisher, USA) to remove residual DNA. After DNase I treatment RNA samples were purified with the CleanRNA Standard kit (Evrogen, Russia). Between 500 and 1000 ng of total RNA were used for library preparation. The NEBNext II Directional RNA Library Prep Kit for Illumina (New England Biolabs, USA) with Poly (A) mRNA Magnetic Isolation Module (New England Biolabs, USA) was employed to convert isolated mRNA into directional strand-specific libraries for sequencing with the "GenoLab M" instrument (GeneMind Biosciences Company, China), a platform, similar to a more widespread "NovaSeq 6000" from Illumina[18]. Libraries were barcoded with dual index primers for pooled sequencing (Multiplex Oligos for

Illumina, New England Biolabs, USA). Sequencing was performed in a 2 $\times$ 150 base pair mode, targeting 10–20 million reads per sample.

Obtained FASTQ files were trimmed with Trim Galore (v0.6.2) and then aligned to the GRCh38 reference genome by STAR (v2.7.10b) with the "-quantMode TranscriptomeSAM" option using Ensembl's v109 transcriptome annotation and quantified with Salmon (v1.10.2). The analysis for differentially expressed genes was performed with the "DESeq2" R package (v1.36.0)[19]. Gene Set Enrichment Analysis (GSEA) was performed with "msigdb" and "clusterProfiler" R packages with default parameters on a list of genes, ordered by  $-\log$  (p-level, adjusted) \* sign (FC), where p-values and FC (fold change of expression) were taken from the DESeq2 results. Cell-type fractions were inferred with a containerized form of CIBERSORTx[20] with the default parameters. RNA-seq counts were transformed to CPM and reference count matrices were left as is. As a reference, we utilized the pancreas portion of a benchmark resource of single-cell RNA-seq human data[21]. Raw counts were extracted with the "scanpy" package (v1.9.5) in Python, only counts originating from the 10X experiments were used.

## Results

### Isolation and immortalization of human PD-MSCs

Human adult pancreatic tissue was enzymatically digested, and the resulting islet subpopulation was separated using Ficoll density gradient centrifugation. The fraction comprising islets, along with a contingent of exocrine cells, was cultured under standard conditions in DMEM supplemented with 10% FBS (Fig. 1A). Following several days of cultivation, islets adhered to the culture surface giving rise to elongated spindle-shaped fibroblast-like cells resembling the classical morphology of MSCs while exocrine cells and other islet cells failed to attach to the culture surface resulting in cell death (Fig. 1B, C, Supplementary Figure S1). Cells were cultivated until reaching 90% confluency, and subsequently, were passaged by trypsin–EDTA treatment. The spindle shape morphology was preserved throughout numerous passages (Fig. 1D). We further decided to immortalize the PD-MSCs to facilitate future studies, as non-immortalized MSCs undergo changes in phenotype and differentiation potential, which are associated with an increased risk of cellular alterations and senescence [22]. After a couple of passages, the cells were transduced with lentivirus harboring human Telomerase Reverse Transcriptase (hTERT) construct to ensure stable expression of *hTERT* cDNA (Supplementary Figure S2), subsequent positive selection based on puromycin resistance was employed for two passages. Both immortalized and non-immortalized cells were cultured under uniform conditions.

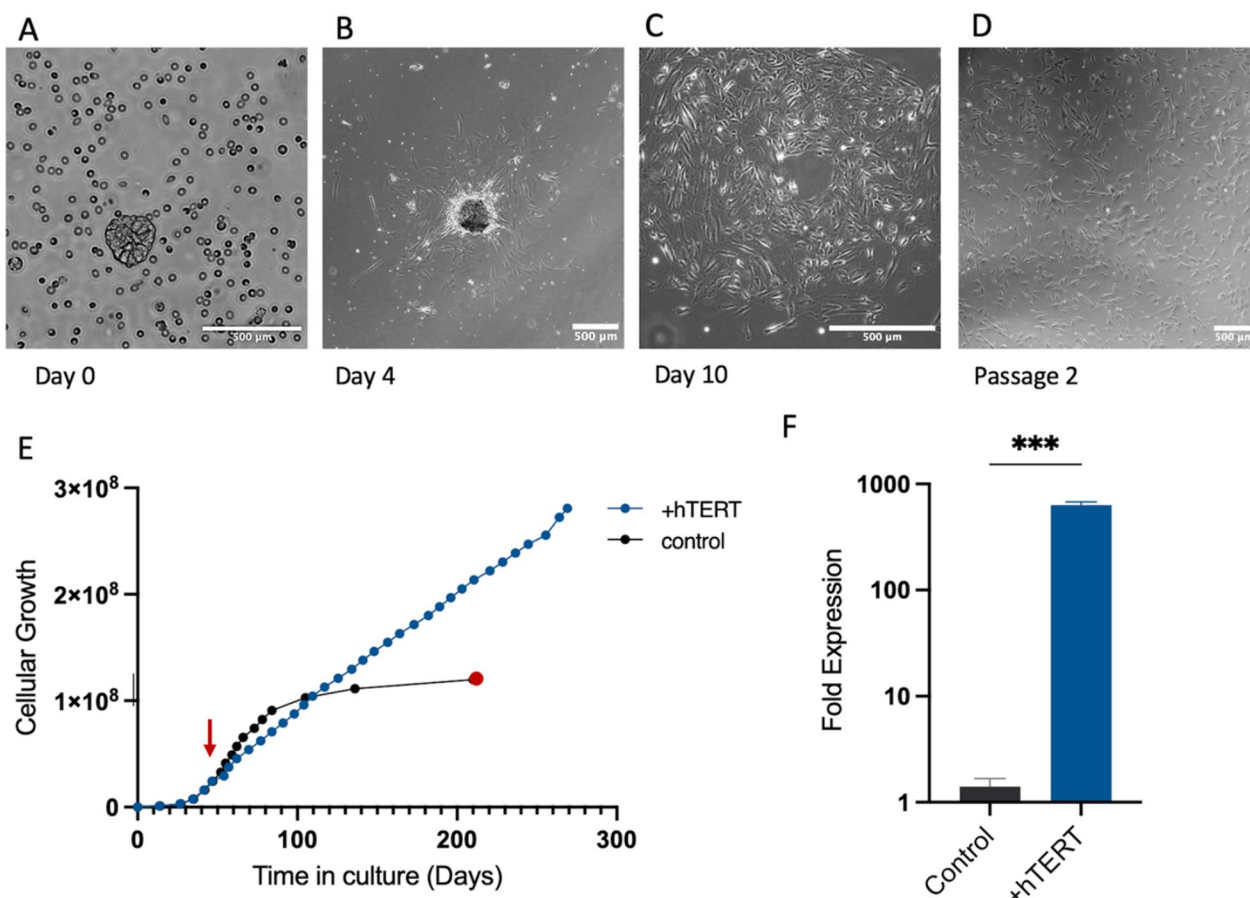


**Fig. 1** Isolation and immortalization of hPD-MSCs. **(A)** Phase-contrast micrograph depicting human pancreatic islets post-isolation, enveloped by adjacent exocrine cells. **(B)** Isolated islets adhere to the culture surface, with cellular growth evident on the outer layer. **(C)** The islet structure dissipated, giving way to cells attaching to the culture surface. **(D)** Subsequent cellular morphology was observed after several passages, illustrating the evolving characteristics during the cultivation process. **(E)** The proliferation rates of three averaged cell lines, comparing both immortalized and non-immortalized cell lines. The red vertical arrow indicates the moment of LV-hTERT transduction, while the red circle marks the point at which proliferation ceased. **(F)** RT-qPCR results for mRNA hTERT in PD-MSCs are depicted before and after immortalization, presented as the average of three independent repeats with standard deviations. Statistical significance was assessed using a paired student's t-test, where  $***P < 0.001$

Non-hTERT-transduced cells exhibited a gradual cessation of proliferation, leading to cell death around 80–100 days (at passage 15), while hTERT-transduced cells sustained proliferative activity, persisting up to 60 passages at the time of manuscript preparation (Fig. 1E). The presence of *hTERT* cDNA was additionally validated using RT-qPCR, hTERT mRNA was significantly higher in immortalized cells compared to non-immortalized control (Fig. 1F).

#### Human pancreas-derived stromal cells display classical mesenchymal features

Isolated cells, whether immortalized or non-immortalized, attach to the culture surface, assuming a fibroblast-like morphology across passages from early to late stages. Subsequently, the expression of established mesenchymal stromal cell markers in hPD-MSCs was investigated

through flow cytometry analysis conducted on both immortalized (late passages 30–35) and non-immortalized cell populations (early passages 2–5). Both immortalized and non-immortalized hPD-MSCs showed strong positive expression of classical MSC markers like CD90, CD106, CD105, CD44, and CD73 (Fig. 2A, B). There was no significant difference between immortalized and non-immortalized hPD-MSCs from different donors (Supplementary Figure S3). Furthermore, in line with the characteristic attributes of mesenchymal stromal cells, hPD-MSCs demonstrated the capacity for differentiation into lineage-specific cell phenotypes under defined growth conditions. Specifically, these cells were cultured in adipogenic and osteogenic media, and subsequently stained with Oil Red O for adipocytes and Alizarin Red S for osteocytes (Fig. 2C, D). These collective findings affirm the classical characteristics of MSCs, establishing

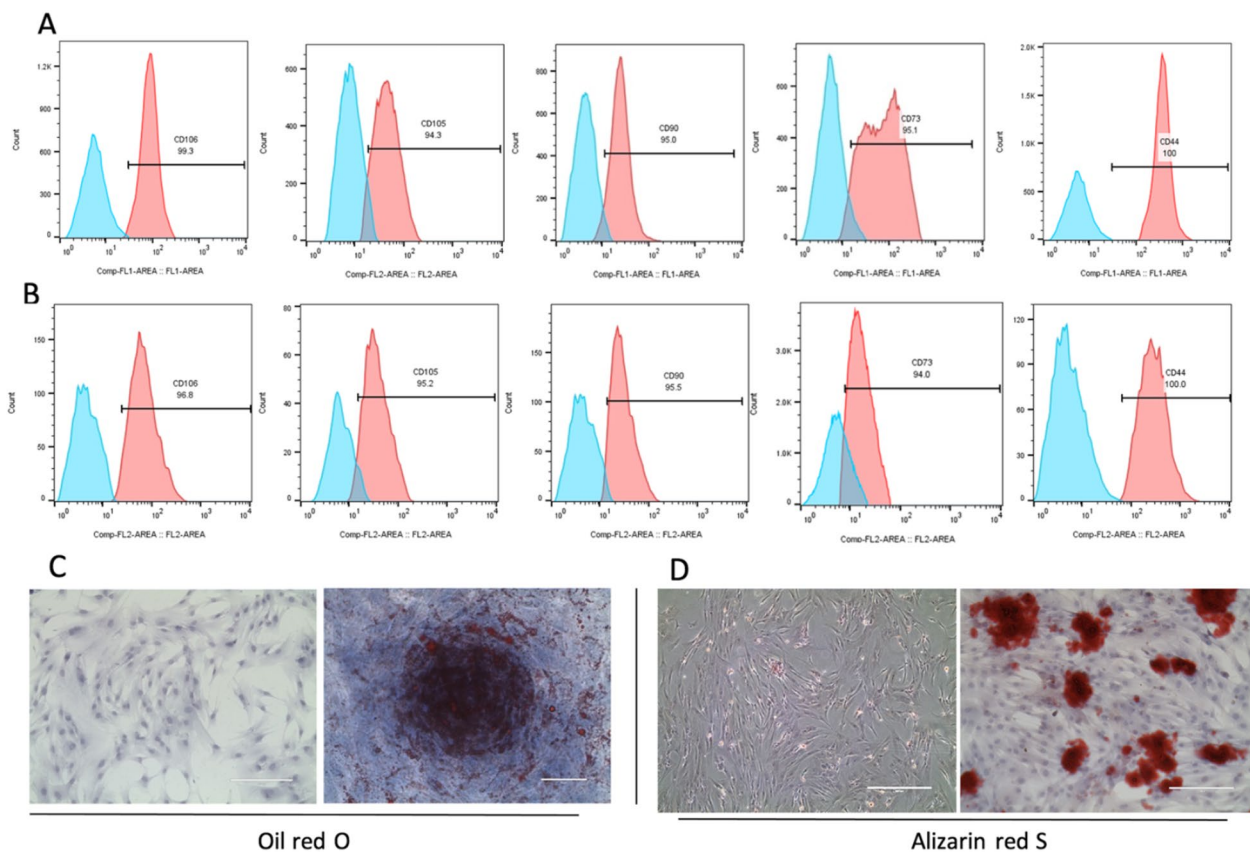


**Fig. 2** Expression of mesenchymal stromal cell markers in PD-MSCs and their multilineage differentiation. **(A, B)** Representative flow cytometric analysis of immortalized and non-immortalized hPD-MSCs samples respectively, showing the specific expression of mesenchymal stromal cell markers CD106, CD105, CD90, CD73, and CD44. **(C)** Adipogenic differentiation of PD-MSCs compared to non-induced control, lipid droplet formation achieved through phase-contrast microscopy and staining with Oil Red O, enhanced with trypan blue. **(D)** Osteogenic differentiation of PD-MSCs compared to non-induced control, The deposition of calcified and mineralized extracellular matrix is visualized by phase-contrast microscopy and staining with Alizarin red S enhanced with trypan blue

hPD-MSCs as a member of the mesenchymal stromal cell category.

#### PD-MSCs share markers of stem cells and pancreatic stellate cells

Mesenchymal stromal cells express pluripotency-related genes that are implicated in self-renewal and cell proliferation, notably, this expression tends to diminish over prolonged culture periods [23]. Key genes implicated in these processes include *KLF4*, *OCT4*, *NANOG*, *SOX2*, *REX1*, *CD44*, and *VCAM1* [23–26]. To further elucidate the stemness characteristics of PD-MSCs, we conducted a comparative analysis using RT-qPCR to assess the expression levels of these markers. Our data indicate no significant disparity in the expression levels of *SOX2*, *OCT4*, and *NANOG* between BM-MSCs and PD-MSCs. BM-MSCs exhibit heightened expression of *REX1*, *VCAM1*, and *CD44* compared to PD-MSCs, underscoring potential differences in their functional properties.

Conversely, PD-MSCs demonstrate elevated expression of *KLF4* relative to BM-MSCs. Moreover, the immortalization process of PD-MSCs leads to enhanced expression of *OCT4* and *KLF4*, suggesting a potential augmentation of stemness-associated pathways upon immortalization. In contrast, adipose tissue-derived mesenchymal stromal cells (AT-MSCs) exhibit higher expression levels of *SOX2*, *CD44*, *REX1*, *OCT4*, and *KLF4* compared to both BM-MSCs and PD-MSCs (Fig. 3A). These results suggest that PD-MSCs, AT-MSCs, and BM-MSCs display similar expression levels of specific pluripotency-related genes. However, variations exist among them, underscoring distinct stem cell attributes inherent to cells derived from diverse tissue origins.

Moreover, our investigation revealed shared characteristics between PD-MSCs and pancreatic stellate cells (PSCs). In vivo, PSCs can exist in two states, activated and quiescent; accordingly, their morphological appearance and expression profile change [27]. Isolated PSCs

initially exist in a quiescent state characterized by the presence of cytoplasmic lipid droplets rich in vitamin A, along with the expression of intermediate filament proteins like Desmin and glial fibrillary acidic protein (GFAP). Upon culturing for a few days, these cells transition into an activated state, marked by the absence of lipid droplets, the upregulation of  $\alpha$ -smooth muscle actin ( $\alpha$ -SMA), and the secretion of ECM proteins [28, 29]. In our study, we measured the expression of Lecithin retinoyl acyltransferase (LRAT), the key enzyme responsible for retinyl ester synthesis and which serves as an important marker of pancreatic stellate cells (Fig. 3B). We also observed positive expressions of  $\alpha$ -SMA, Nestin, Desmin, and ECM components like laminin, fibronectin, decorin, and collagen 1 in PD-MSCs and a lack of GFAP expression (Fig. 3C) indicating a notable resemblance between PD-MSCs and PSCs. Moreover, we have also observed positive staining for CXCL12 which plays a major role in the maintenance, mobilization, and migration of stromal cells [30], and positive staining of neural progenitors' markers ASCL1 and FOXA2 (Supplementary Figure S4).

#### Comparison of transcriptomic profiles of obtained mesenchymal stromal cells

To further characterize PD-MSCs, we performed RNA-seq experiments on 5 original PD-MSCs samples, 3 immortalized PD-MSCs, 3 AT-MSCs, and 3 BM-MSCs samples. We obtained on average 5.5 million (minimum 4.3 million) mapped reads for the analysis. The direct comparison of the original PD-MSCs with the iPDMSCs (Supplementary Table S3) revealed an expected enrichment in differentially expressed genes of mitotic processes (such as "DNA-dependent DNA Replication",  $p$ -value =  $4.4e-08$ ), as well as genes involved in cell response to foreign DNA (such as "Negative Regulation of Viral Genome Replication",  $p$ -value =  $1.0e-07$ ), likely caused by the transduction method (Supplementary Table S4). On the other hand, both original and immortalized cells seem to be more similar to each other than to both AT-MSCs and BM-MSCs (Fig. 4A). The expression of established mesenchymal cell markers indicated that PD-MSCs exhibit similar expression profiles for mesenchymal markers as AT-MSCs and BM-MSCs (Fig. 4B).

Moreover, we conducted a more precise comparison with the tissue of origin, the pancreatic scRNA-seq

dataset from the Tabula Sapiens experiment [21] via a digital cytometry method, CIBERSORTx[20]. Across all cell types, the correlation with reference data is weak, averaging 0.15 for PD-MSCs and even lower (0.08) for other AT-MSCs and BM-MSCs, indicating that in vitro PD-MSC lost their original identity of the source material. However, this comparison allowed us to pinpoint a significantly higher similarity between hPD-MSCs and pancreatic stellate cells, whereas AT-MSCs and BM-MSCs showed greater resemblance to fibroblast populations rather than PSCs (Fig. 4C, Supplementary Table S5). The Tabula Sapiens pancreatic dataset contains three clusters of stellate cells: quiescent, activated, and an unspecified additional cluster (Supplementary Figure S6A). Notably, the CIBERSORTx analysis predominantly identifies PD-MSCs within the unspecified stellate cell cluster, while for AT-MSCs and BM-MSCs, pancreatic fibroblasts seem to be the most similar cell type.

Next, we tried to find genes whose expression would be characteristic of PD-MSCs. To minimize false positives, we tested original and immortalized PD-MSCs against AT-MSCs and BM-MSCs separately in four analyses for differentially expressed genes (DEG) (Supplementary Table S6). We found that there are 26 differentially expressed genes with effect  $\log_2FC > 2$  and a  $p$ -value (BH-adjusted)  $< 0.05$  (Fig. 4D) in all four analyses. Among them are genes of 1) transcription factors and transcription regulation (*FOXE1*, *FOXF1*, *HOXB-AS3*, *TCF21*, *ZNF804A*), 2) enzymes and enzyme regulators (*PLAT*, *PPP1R14*, *ALDH1A1*, *EDN1*), 3) channels and other membrane proteins (*ANO1*, *CHRM2*, *COL4A5*, *SCN9A*, *SYT1*), 4) proteins involved in signal transduction (*CORIN*, *GPR37*, *IGF2BP1*, *KIT*, *NPTX1*, *RGS7*), and 5) with other or undefined function (*COLEC10*, *C8orf34*, *CD163L1*, *LRRC2*, *RTN1*, and a gene without the HGNC symbol: *ENSG00000286190*, also known as *LOC728392*) (Fig. 4E). Note, that the novel gene was added in the Ensembl annotation files since release 96 (2019), and before that, the corresponding transcript was attributed to a nearby gene *NLRP1* (Supplementary Figure S7). Most of these genes whose counts are present in the pancreatic Tabula Sapiens dataset, are found in stellate cells, however, not exclusive for any of its subtypes, which is in line with our CIBERSORTx analysis (Supplementary Fig. 6B). The selective expression of some of these genes

(See figure on next page.)

**Fig. 3** Expression of stemness and PSCs markers in PD-MSCs. **(A)** RT-qPCR results comparing the expression levels of stemness markers in PD-MSCs relative to iPDMSCs, BM-MSCs, and AT-MSCs. **(B)** RT-qPCR results comparing the expression levels of LRAT enzyme in PD-MSCs compared to iPDMSCs, BM-MSCs, AT-MSCs- human fibroblasts. Data presented as an average of at least 3 biological repeats with standard deviation, statistical significance was assessed using ANOVA analysis where \* $P < 0.033$ , \*\* $P < 0.0021$ , \*\*\* $P < 0.0002$ , \*\*\*\* $P < 0.0001$ . **(C)** immunocytochemistry staining results of PSCs markers in PD-MSCs including CXCL12, Desmin, Laminin, Nestin,  $\alpha$ -SMA, GFAP, Fibronectin, Decorin, Collagen I

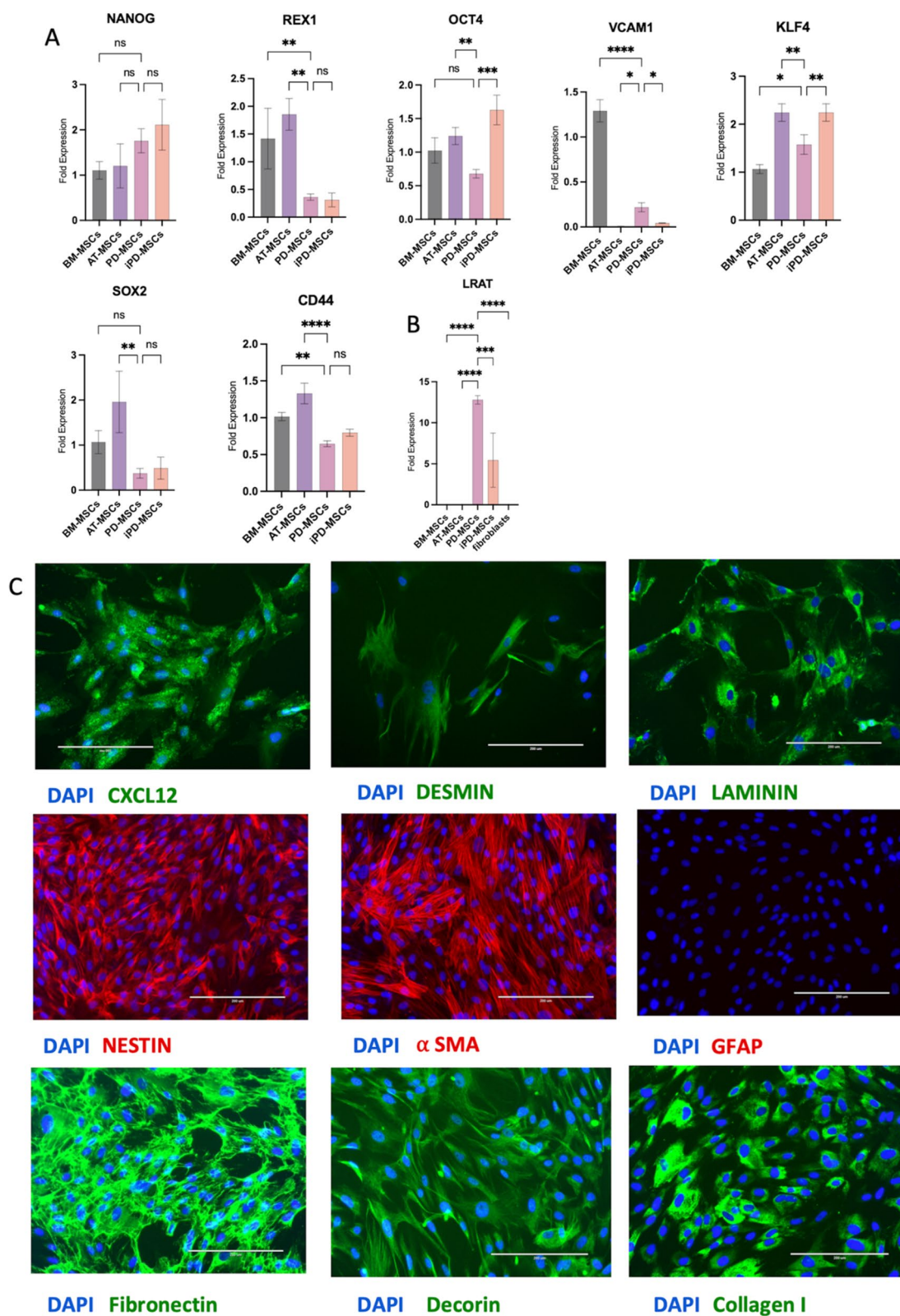


**Fig. 3** (See legend on previous page.)



was also evaluated by RT-qPCR, the results are in agreement for all of the tested genes (Fig. 5).

Additionally, we verified the distinctive expression in PD-MSCs of *ISL1*. Despite its overall low expression, it remains significantly higher in PD-MSCs than in AT-MSCs and BM-MSCs. It is important to note that, in our DEG analysis, we were unable to demonstrate statistical significance for *ISL1* when comparing immortalized PD-MSCs with AT-MSCs ( $P_{adj}=0.1$ ), other comparisons being significant ( $P_{adj}<0.05$ ) and an increase in expression was observed for all models (see Supplementary Table S6).

System analysis yielded little enrichment, probably due to the limited number of samples. Gene set enrichment analysis (GSEA) on DEG for the four tested models (Supplementary Tables S7-10) revealed three common ontology sets with adjusted  $p$ -value  $<0.05$ : “Skeletal System Development”, “Bone Morphogenesis”, and “Bone Development”. According to the GSEA’s normalized enrichment score, all of these processes are suppressed in PD-MSCs.

## Discussion

MSCs exhibit the ability to differentiate into diverse cell types and play a crucial role in modulating immune responses, impacting both the adaptive and innate immune systems [31, 32]. The significance of these findings has garnered substantial attention over the last decade, highlighting the potential applications of MSCs in the treatment of numerous diseases. Although MSCs were initially derived from bone marrow, they can be isolated from almost all tissues [33], which is reflected in the recent clinical trials including MSC products [34]. Despite the rapid progress in this field, irritations remain concerning the defining characteristics of these cells, including their differentiation potency, self-renewal, and in vivo properties [32]. Culture-expanded MSCs unavoidably consist of a heterogeneous population whereas the degree of heterogeneity varies depending on the isolation technique, culturing protocols, culture media, passage number as well as tissue origin [35, 36]. As a consequence, the MSCs acronym has been collectively referred to as mesenchymal stem cells, multipotential stromal cells, and mesenchymal stromal cells [31], which generated a growing tendency to challenge this

term, especially with respect to stem cell characteristics. In 2005, the International Society for Cellular Therapy issued a position statement containing a minimal criterion to define MSCs and clarifying that the term mesenchymal stem cell is not equivalent or interchangeable with mesenchymal stromal cell (MSC) [37]. However, the interchangeable use of MSCs as mesenchymal stem cells or mesenchymal stromal cells has since propagated. Unsurprisingly, MSCs isolated from the pancreas have been subjected to the same terminology discrepancy, Mesenchymal stromal cells of the pancreas appear in literature under many names, including mesenchymal stromal cells, mesenchymal stem cells, pancreatic stem cells, and possibly pancreatic stellate cells [6, 8–10, 38, 39]

To meet the criteria for the designation of MSCs, culture-expanded cells must exhibit the following attributes: (1) adherence to plastic substrates, (2) expression of CD105, CD73, and CD90 while lacking hematopoietic surface markers, and (3) demonstrable in vitro differentiation capacity into osteoblasts, adipocytes, and chondroblasts [37]. Our findings suggest that fibroblast-like cells derived from pancreatic islets exhibit morphological characteristics similar to MSCs, express CD105, CD73, CD90, and CD44, and successfully undergo in vitro differentiation into adipocytes and osteocytes. These observations align with the criteria for the classification of mesenchymal stromal cells, hereby denoted as PD-MSCs. Additionally, our findings reveal a positive expression of CD106, also known as vascular cell adhesion molecule 1 (VCAM-1). CD106 is recognized for its pivotal role in provoking effective immune responses, including T-cell activation and leukocyte recruitment, as well as contributing to MSC-mediated immunosuppression [40]. Notably, CD106 has been identified as a marker of MSCs isolated from BM, chorionic villi, and umbilical cord and as a component within the neural stem cell niche [41]. Moreover, we confirmed the presence of VCAM-1 among other stemness-related genes RT-qPCR, comparable expression levels of these genes were observed across all types of mesenchymal cells, with variations attributed to their tissue of origin. Specifically, AT-MSCs exhibited higher expression of SOX2 and CD44, whereas BM-MSCs demonstrated elevated levels of VCAM1.

(See figure on next page.)

**Fig. 4** Transcriptomic analysis of PD-MSCs. **(A)** Principal components plot for the variance stabilized counts of the obtained transcriptomes of PD-MSCs, iPD-MSCs, AT-MSCs, and BM-MSCs. **(B)** Heatmap of log-transformed transcripts per million (TPMs) of genes of various pancreatic markers for the studied MSCs samples. **(C)** Inferred proportions of pancreatic cells and correlation of the RNA-seq samples with the pancreatic Tabula Sapiens dataset by the CIBERSORTx. **(D)** Venn diagram of intersection of statistically meaningful ( $P_{adj}<0.05$ ) DEG with big effects ( $\log_2FC>2$ ) for PD-MSCs, original and immortalized (denoted as “iPD”) separately, vs BM-MSCs (blue) and AT-MSCs (green). **(E)** Heatmap of log-transformed transcripts per million (TPMs) of PD-MSCs-specific genes for the studied MSCs samples

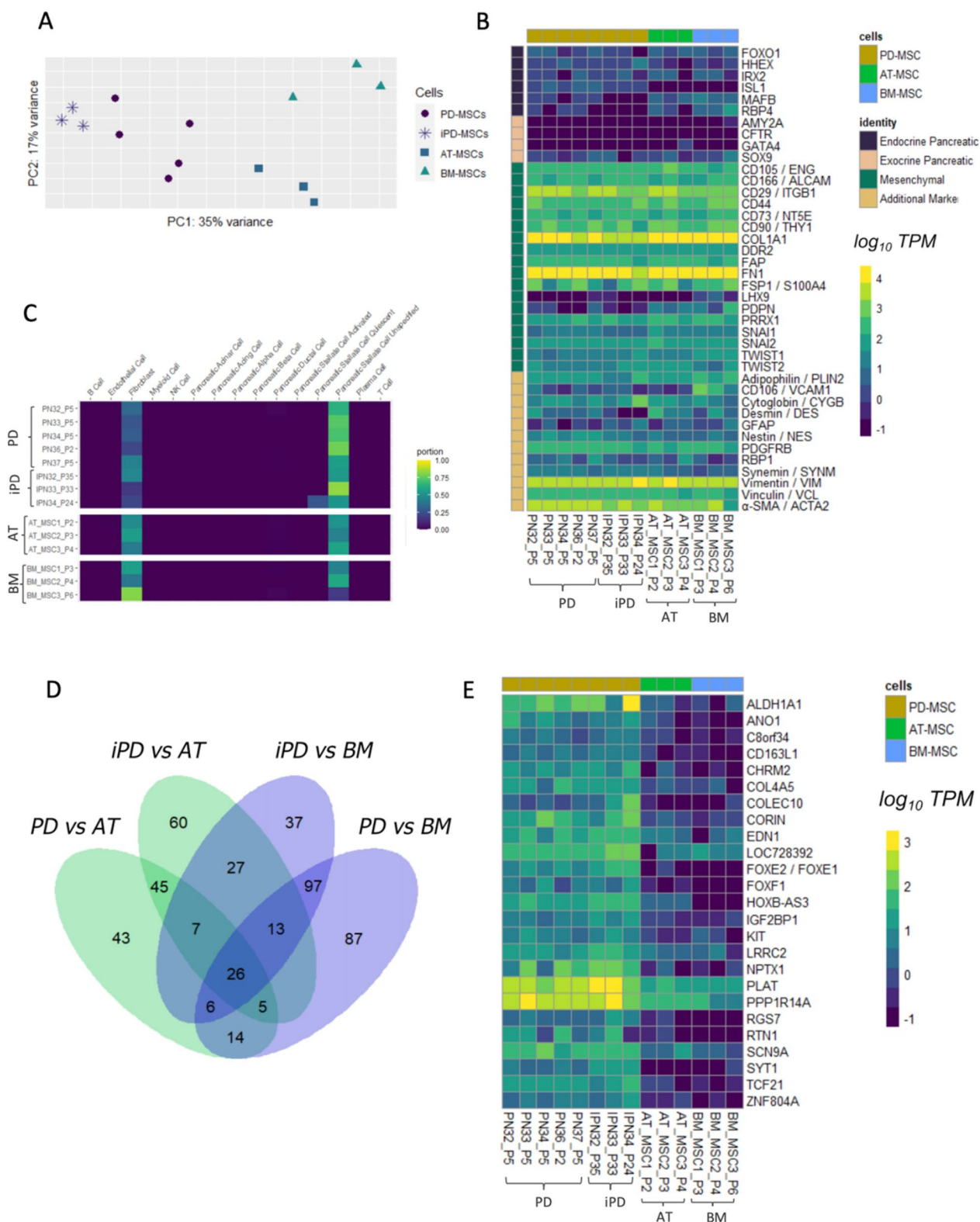


**Fig. 4** (See legend on previous page.)

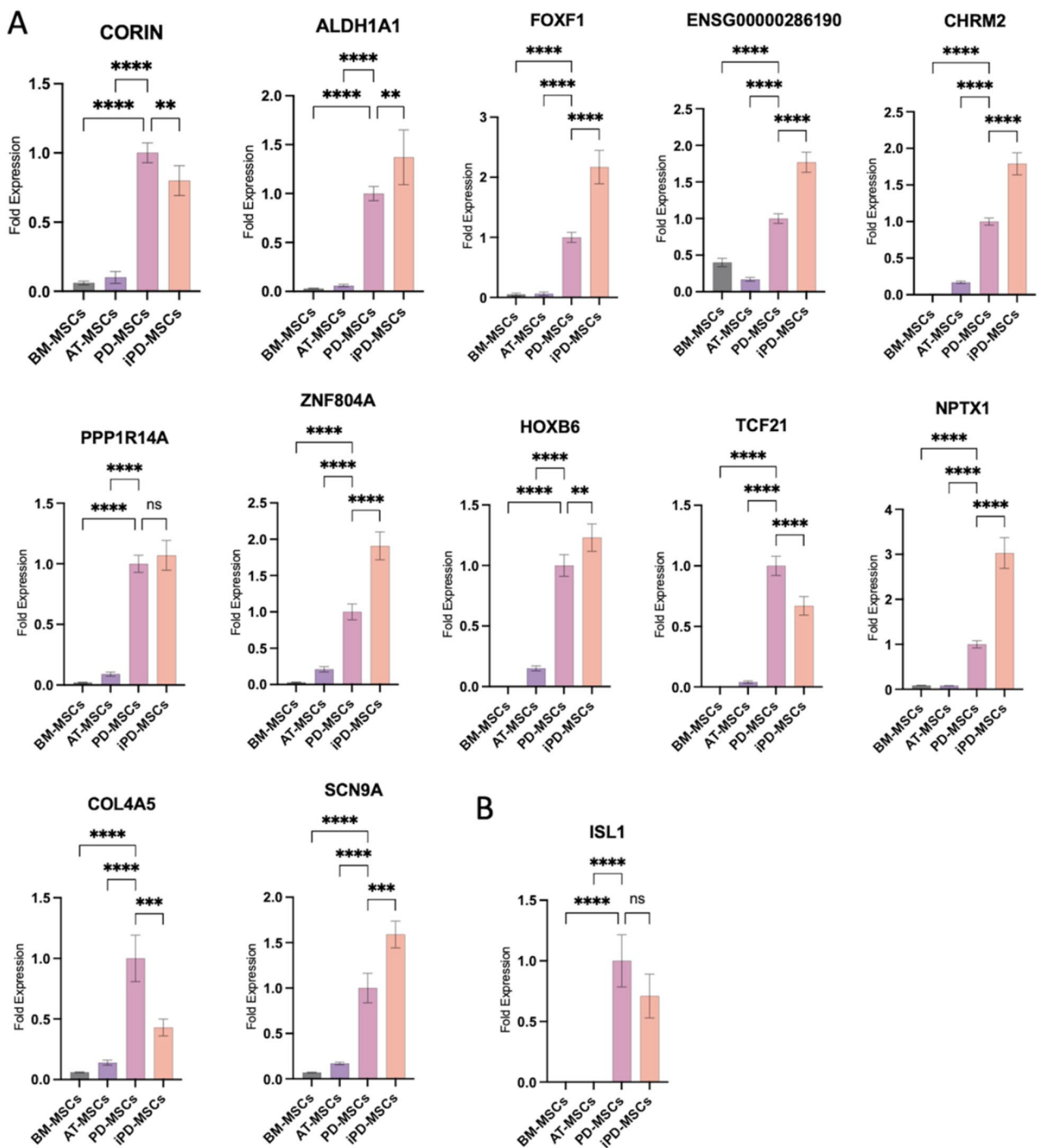


**Fig. 5** (A) Verification of transcriptome results by RT-qPCR in PD-MSCs compared to iPD-MSCs, BM-MSCs, and AT-MSCs. (B) expression of ISL1 in PD-MSCs and iPD-MSCs compared to BM-MSCs and AT-MSCs. Data presented as an average of at least 3 biological repeats with standard deviation, statistical significance was assessed using ANOVA analysis where \*\* $P < 0.0021$ , \*\*\* $P < 0.0002$ , and \*\*\*\* $P < 0.0001$

According to our digital cytometry analysis, transcriptomes of PD-MSCs are more similar to transcriptomes of Pancreatic Stellate Cells (PSCs) than AT- and BM-MSCs. PSCs represent a versatile cell type constituting

approximately  $4.78 \pm 0.74\%$  of the total cells in the exocrine part and  $0.14 \pm 0.015\%$  of total cells in islets [42, 43]. In vivo, PSCs exhibit two distinct states: quiescent and activated. In their quiescent state, PSCs feature

intracellular lipid droplets and express GFAP, Nestin, and Desmin. Upon activation, PSCs transition into myofibroblast-like cells, lipid droplets disappear, and PSCs upregulate  $\alpha$ -SMA, and secrete extracellular matrix components, thereby contributing to pancreatic fibrosis [27]. The activation of PSCs is governed by multiple signaling pathways [44], which makes it difficult to determine their precise state in vitro. Of note, the analysis points to the uncharacterized “Unspecified Pancreatic Stellate Cell” from the Tabula Sapiens annotation. From the scRNA-seq data itself, it is hard to say whether this distinct cell type represents a specific type of functional PSCs or just a pool of immature PSCs or intermediary cells between activated and quiescent PSCs. PSCs have been reported to resemble hepatic stellate cells, which not only express mesenchymal cell markers, but also neural cell markers, including nestin, GFAP, and p75 neurotrophin receptor [45, 46]. Moreover, PSCs isolated from mice show morphological resemblance to MSCs but are functionally distinct, showing higher expression of paracrine factors and enhancing glucose-induced insulin secretion when co-cultured with islets [47]. Recently, PSCs have garnered attention as potential pancreatic stem cells, given their proximity to islets, expression of diverse stem cell markers, and demonstrated multipotent differentiation capabilities including the generation of insulin-producing cells [46]. On the other hand, another study suggested PSCs play a negative role in the differentiation of  $\beta$ -cells during pancreas development, suggesting that the manipulation of PSC activity could be a useful tool during the development of cell-based therapies for the treatment of diabetes. Our study highlights the resemblance between PD-MSCs and PSCs represented by the expression of LRAT, and other PSCs markers including  $\alpha$ -SMA, desmin, and ECM components including laminin, fibronectin, decorin, and collagen I.

Additionally, we found 26 genes whose expression differentiates PD-MSCs from other mesenchymal cells. One of these genes is *ALDH1A1*, which encodes an enzyme that converts retinaldehyde to retinoic acid. This gene is expected to be expressed in PSCs. Moreover, one of the features of pancreatic stellate cells is the ability to store retinoic acid [48] which is known to be a major transformation agent of cells towards the neuronal niche [49]. Therefore, it is not surprising that at least seven PD-MSCs-specific genes are more characteristic of neurons than mesenchymal cells (*CHRM2*, *GPR37*, *NPTX1*, *RGS7*, *SCN9A*, *SYT1*, *ZNF804A*), although the reasons for the enrichment of each of these genes in pancreatic mesenchymal cells remain unclear. For instance, *ZNF804A*, a transcription factor that regulates neurite outgrowth, is predominantly known as a genetic risk factor for schizophrenia and bipolar disorder [50]. However, no functions related to pancreatic processes for this gene have yet been

established. Another interesting result was the identification of the novel gene *ENSG00000286190* (*LOC728392*) among the DEGs for PD-MSCs. The function of this gene is unknown, except that it is predominantly expressed in brain and endocrine tissues [51]. Previously, a transcript from this gene was thought to belong to the nearby *NLRP1* gene. It is possible that some findings attributed to *NLRP1*, such as its role as a biomarker for pancreatic cancer [52, 53], could be related to this novel gene. Notably, we did not observe positive expression of endocrine markers in all mesenchymal cells, except for *ISL1*, which is an essential endocrine transcription factor for the survival and differentiation of pancreatic endocrine progenitors [54]. This gene expresses higher in PD-MSCs and iPD-MSCs compared to other mesenchymal cell types, reaching a significance level ( $P_{adj} < 0.05$ ) for DEG in three out of four tested models, validated via RT-qPCR. The distinct neuronal signatures that we get from PD-MSCs, in comparison with other MSCs, could be interpreted as these cells having a Neural Crest (NC) origin. Indeed, cells originating from the NC were found in the pancreas of mice [55], where they supposedly regulate the growth of the islets [56]. While it is tempting to suggest that our PD-MSCs originate from such cells, we don't see NC-specific markers in PD-MSCs.

Despite advancements in MSC research, significant challenges persist in their characterization, largely stemming from the heterogeneous nature of culture-expanded MSC populations and the variability arising from factors such as tissue origin, culture method, and donor specificity. Pancreas-derived MSCs show promise in addressing pancreatic pathologies, prompting a comprehensive characterization effort. Our study sheds light on the similarities and differences between PD-MSCs and other mesenchymal cell types. We confirmed typical MSC characteristics in PD-MSCs and identified neural niche markers, suggesting a resemblance to pancreatic stellate cells. Further investigation is necessary to grasp the functional implications of these findings and explore the therapeutic potential of PD-MSCs. This integrated approach will enhance our understanding of PD-MSCs and their role in advancing regenerative medicine and cell therapy.

## Conclusions

This study provides a detailed characterization of PD-MSCs, highlighting their similarities to MSCs of other origins and to PSCs. PD-MSCs demonstrate the expected MSC characteristics including classical surface markers, and the ability to differentiate into adipocytes and osteocytes. Additionally, the expression of neural niche markers and their resemblance to pancreatic stellate cells

(PSCs) suggest that PD-MSCs may share a functional relationship with these cells.

Our findings also reveal that PD-MSCs exhibit a distinctive gene expression profile, with some genes typically associated with neural functions and others potentially linked to pancreatic processes. However, the heterogeneity of MSC populations, influenced by factors such as tissue origin and culture conditions, continues to pose challenges in their precise characterization. Further research is needed to elucidate the functional roles of PD-MSCs, particularly in relation to their neural and pancreatic characteristics. Understanding these aspects could unlock new therapeutic potentials for PD-MSCs, especially in the context of treating pancreatic diseases and exploring their broader application in regenerative medicine and cell therapy.

#### Abbreviations

AT-MSCs	Adipose tissue-derived mesenchymal stromal cells
BM-MSCs	Bone marrow-derived mesenchymal stromal cells
FBS	Fetal bovine serum
hPD-MSCs	Human pancreas-derived mesenchymal stromal cells
hTERT	Human telomerase reverse transcriptase
iPD-MSCs	Immortalized pancreas-derived mesenchymal stromal cells
PSCs	Pancreatic stellate cells
RT-qPCR	Reverse transcription quantitative polymerase chain reaction
DEG	Differentially expressed genes
GSEA	Gene set enrichment analysis

#### Supplementary Information

The online version contains supplementary material available at <https://doi.org/10.1186/s13287-024-03963-2>.

Additional file 1.

Additional file 2.

#### Acknowledgements

The authors declare that they have not use AI-generated work in this manuscript.

#### Author contributions

Conceptualization and methodology—EN, DE, TV; Sample collection—EN, TV, AA, IR, DT; Cell biology—EN, DE, KE; Molecular biology—EN, AA, GN, VE, KE; Bioinformatics—KN; Writing—EN, DE, AA, KN; Supervision—DE, GV. All authors have read and agreed to the published version of the manuscript.

#### Funding

This work was supported by a grant No. 075–15-2019–1789 from the Ministry of Science and Higher Education of the Russian Federation allocated to the Center for Precision Genome Editing and Genetic Technologies for Biomedicine.

#### Availability of data and materials

FASTQ files with sequencing reads generated in this study for RNA-seq are available in the SRA database, accession number PRJNA1076671.

#### Declarations

##### Ethics approval and consent to participate

The human pancreatic tail specimens were taken by incision biopsy after distal pancreatectomy or laparoscopic pancreatoduodenectomy in five patients (age  $\geq$  45 yr, M:F = 3:2) diagnosed with pancreatic cancer. This part of the

study was conducted in accordance with the Declaration of Helsinki and the legislation of the Russian Federation on human health protection. The use of biopsied tissue for scientific purposes was approved by the Ethical Board at the Loginov Moscow Clinical Scientific Center (Board Record #1/2020 of February 3, 2020), title of the approved project "Development of technology for reprogramming stromal cells for the treatment of type 1 diabetes". All patients provided written informed consent for biospecimen donation and signed a special agreement for participation in scientific research.

#### Competing interests

The authors declare no conflict of interest. The funders had no role in the design of the study, in the collection, analysis, or interpretation of data, in the writing of the manuscript, or in the decision to publish the results.

#### Author details

<sup>1</sup>Center for Precision Genome Editing and Genetic Technologies for Biomedicine, Pirogov Russian National Research Medical University, Moscow, Russia 117997. <sup>2</sup>Mental Health Research Center, Moscow, Russia 115522. <sup>3</sup>Research Institute of Molecular and Cellular Medicine, RUDN University, Moscow, Russia 117198. <sup>4</sup>Loginov Moscow Clinical Scientific Center, Moscow, Russia 111123. <sup>5</sup>Research Institute for Systems Biology and Medicine, Moscow, Russia 117246. <sup>6</sup>Moscow Institute of Physics and Technology (State University), Dolgoprudny, Russia 141701. <sup>7</sup>Dmitry Rogachev National Medical Research Center of Pediatric Hematology, Oncology and Immunology (D. Rogachev, NMRCPHOI) of Ministry of Healthcare of the Russian Federation, 1, Samory Mashela St, Moscow, Russia 117997. <sup>8</sup>Department of Hospital Surgery, Sklifosovsky Institute for Clinical Medicine, Sechenov First Moscow State Medical University (Sechenov University), Moscow, Russia 119435. <sup>9</sup>Institute of Medicine, Banzarov Buryat State University, Ulan-Ude, Russia 670000.

Received: 16 August 2024 Accepted: 26 September 2024

Published online: 08 October 2024

#### References

- Marcuzzi A, Maximova N. Editorial: advances in stem cell therapy: new applications and innovative therapeutic approaches. *Front Med*. 2023;10:1225551.
- Berebichez-Fridman R, Montero-Olvera PR. Sources and clinical applications of mesenchymal stem cells: state-of-the-art review. *Sultan Qaboos Univ Med J*. 2018;18:e264–77.
- Hass R, Kasper C, Böhm S, Jacobs R. Different populations and sources of human mesenchymal stem cells (MSC): a comparison of adult and neonatal tissue-derived MSC. *Cell Commun Signal*. 2011;9:12.
- Kozłowska U, Krawczenko A, Futoma K, Jurek T, Rorat M, Patrzalek D, et al. Similarities and differences between mesenchymal stem/progenitor cells derived from various human tissues. *World J Stem Cells*. 2019;11:347–74.
- Stanko P, Kaiserova K, Altanerova V, Altaner C. Comparison of human mesenchymal stem cells derived from dental pulp, bone marrow, adipose tissue, and umbilical cord tissue by gene expression. *Biomed Pap Med Fac Univ Palacky Olomouc Czech Repub*. 2014;158:373–7.
- Seeberger KL, Dufour JM, Shapiro AMJ, Lakey JRT, Rajotte RV, Korbitt GS. Expansion of mesenchymal stem cells from human pancreatic ductal epithelium. *Lab Invest*. 2006;86:141–53.
- Lee S, Jeong S, Lee C, Oh J, Kim S-C. Mesenchymal stem cells derived from human exocrine pancreas spontaneously express pancreas progenitor-cell markers in a cell-passage-dependent manner. *Stem Cells Int*. 2016;2016:2142646.
- Khiatah B, Qi M, Du W, T-Chen K, van Megen KM, Perez RG, et al. Intra-pancreatic tissue-derived mesenchymal stromal cells: a promising therapeutic potential with anti-inflammatory and pro-angiogenic profiles. *Stem Cell Res Ther*. 2019;10:322.
- Thirlwell KL, Colligan D, Mountford JC, Samuel K, Bailey L, Cuesta-Gomez N, et al. Pancreas-derived mesenchymal stromal cells share immune response-modulating and angiogenic potential with bone marrow mesenchymal stromal cells and can be grown to therapeutic scale under good manufacturing practice conditions. *Cytotherapy*. 2020;22:762–71.
- Villard O, Armanet M, Couderc G, Bory C, Moreaux J, Noël D, et al. Characterization of immortalized human islet stromal cells reveals a MSC-like profile with pancreatic features. *Stem Cell Res Ther*. 2020;11:158.

11. Sordi V, Melzi R, Mercalli A, Formicola R, Dogliani C, Tiboni F, et al. Mesenchymal cells appearing in pancreatic tissue culture are bone marrow-derived stem cells with the capacity to improve transplanted islet function. *Stem Cells*. 2010;28:140–51.
12. De Waele E, Wauters E, Ling Z, Bouwens L. Conversion of human pancreatic acinar cells toward a ductal-mesenchymal phenotype and the role of transforming growth factor  $\beta$  and activin signaling. *Pancreas*. 2014;43:1083–92.
13. Baertschiger RM, Bosco D, Morel P, Serre-Beinier V, Berney T, Buhler LH, et al. Mesenchymal stem cells derived from human exocrine pancreas express transcription factors implicated in beta-cell development. *Pancreas*. 2008;37:75–84.
14. Mehigan DG, Bell WR, Zuidema GD, Eggleston JC, Cameron JL. Disseminated intravascular coagulation and portal hypertension following pancreatic islet autotransplantation. *Ann Surg*. 1980;191:287–93.
15. Ricordi C, Lacy PE, Finke EH, Olack BJ, Scharp DW. Automated method for isolation of human pancreatic islets. *Diabetes*. 1988;37:413–20.
16. Stull ND, Breite A, McCarthy R, Tersey SA, Mirmira RG. Mouse islet of Langerhans isolation using a combination of purified collagenase and neutral protease. *J Vis Exp*. 2012. <https://doi.org/10.3791/4137>.
17. Evtushenko NA, Beilin AK, Dashinimaev EB, Ziganshin RH, Kosykh AV, Perfilov MM, et al. hTERT-driven immortalization of RDEB fibroblast and keratinocyte cell lines followed by cre-mediated transgene elimination. *Int J Mol Sci*. 2021. <https://doi.org/10.3390/ijms22083809>.
18. Liu Y, Han R, Zhou L, Luo M, Zeng L, Zhao X, et al. Comparative performance of the GenoLab M and NovaSeq 6000 sequencing platforms for transcriptome and lncRNA analysis. *BMC Genomics*. 2021;22:829.
19. Love MI, Huber W, Anders S. Moderated estimation of fold change and dispersion for RNA-seq data with DESeq2. *Genome Biol*. 2014;15:550.
20. Newman AM, Steen CB, Liu CL, Gentles AJ, Chaudhuri AA, Scherer F, et al. Determining cell type abundance and expression from bulk tissues with digital cytometry. *Nat Biotechnol*. 2019;37:773–82.
21. Tabula Sapiens Consortium\*, Jones RC, Karkanas J, Krasnow MA, Pisco AO, Quake SR, et al. The Tabula Sapiens: A multiple-organ, single-cell transcriptomic atlas of humans. *Science*. 2022;376:bl4896.
22. Yang Y-HK, Ogando CR, Wang-See C, Chang T-Y, Barabino GA. Changes in phenotype and differentiation potential of human mesenchymal stem cells aging in vitro. *Stem Cell Res Ther*. 2018;9:131.
23. Tantrawatpan C, Manochantr S, Kheolamai P, U-Pratya Y, Supokawej A, Issaragrisil S. Pluripotent gene expression in mesenchymal stem cells from human umbilical cord Wharton's jelly and their differentiation potential to neural-like cells. *J Med Assoc Thai*. 2013;96:1208–17.
24. Seymour T, Twigger A-J, Kakulas F. Pluripotency genes and their functions in the normal and aberrant breast and brain. *Int J Mol Sci*. 2015;16:27288–301.
25. Du W, Li X, Chi Y, Ma F, Li Z, Yang S, et al. VCAM-1+ placenta chorionic villi-derived mesenchymal stem cells display potent pro-angiogenic activity. *Stem Cell Res Ther*. 2016;7:49.
26. Ghaleb AM, Yang VW. Krüppel-like factor 4 (KLF4): what we currently know. *Gene*. 2017;611:27–37.
27. Nielsen MFB, Mortensen MB, Detlefsen S. Identification of markers for quiescent pancreatic stellate cells in the normal human pancreas. *Histochem Cell Biol*. 2017;148:359–80.
28. Zha M, Xu W, Jones PM, Sun Z. Isolation and characterization of human islet stellate cells. *Exp Cell Res*. 2016;341:61–6.
29. Yamamoto G, Taura K, Iwaisako K, Asagiri M, Ito S, Koyama Y, et al. Pancreatic stellate cells have distinct characteristics from hepatic stellate cells and are not the unique origin of collagen-producing cells in the pancreas. *Pancreas*. 2017;46:1141–51.
30. Janssens R, Struyf S, Proost P. The unique structural and functional features of CXCL12. *Cell Mol Immunol*. 2018;15:299–311.
31. Wu X, Jiang J, Gu Z, Zhang J, Chen Y, Liu X. Mesenchymal stromal cell therapies: immunomodulatory properties and clinical progress. *Stem Cell Res Ther*. 2020;11:345.
32. Lindner U, Kramer J, Rohwedel J, Schlenke P. Mesenchymal stem or stromal cells: toward a better understanding of their biology? *Transfus Med Hemother*. 2010;37:75–83.
33. Nombela-Arrieta C, Ritz J, Silberstein LE. The elusive nature and function of mesenchymal stem cells. *Nat Rev Mol Cell Biol*. 2011;12:126–31.
34. Moll G, Ankrum JA, Kamhih-Milz J, Bieback K, Ringdén O, Volk H-D, et al. Intravascular mesenchymal stromal/stem cell therapy product diversification: time for new clinical guidelines. *Trends Mol Med*. 2019;25:149–63.
35. Wilson A, Webster A, Genever P. Nomenclature and heterogeneity: consequences for the use of mesenchymal stem cells in regenerative medicine. *Regen Med*. 2019;14:595–611.
36. Lukomska B, Stanaszek L, Zuba-Surma E, Legosz P, Sarzynska S, Drelich K. Challenges and controversies in human mesenchymal stem cell therapy. *Stem Cells Int*. 2019;2019:9628536.
37. Dominici M, Le-Blanc K, Mueller I, Slaper-Cortenbach I, Marini F, Krause D, et al. Minimal criteria for defining multipotent mesenchymal stromal cells. The International Society for Cellular Therapy position statement. *Cytotherapy*. 2006;8:315–7.
38. Gallo R, Gambelli F, Gava B, Sasdelli F, Tellone V, Masini M, et al. Generation and expansion of multipotent mesenchymal progenitor cells from cultured human pancreatic islets. *Cell Death Differ*. 2007;14:1860–71.
39. Zanini C, Bruno S, Mandili G, Baci D, Cerutti F, Cenacchi G, et al. Differentiation of mesenchymal stem cells derived from pancreatic islets and bone marrow into islet-like cell phenotype. *PLoS ONE*. 2011;6:e28175.
40. Kokovay E, Wang Y, Kusek G, Wurster R, Lederman P, Lowry N, et al. VCAM1 is essential to maintain the structure of the SVZ niche and acts as an environmental sensor to regulate SVZ lineage progression. *Cell Stem Cell*. 2012;11:220–30.
41. Yang ZX, Han Z-B, Ji YR, Wang YW, Liang L, Chi Y, et al. CD106 identifies a subpopulation of mesenchymal stem cells with unique immunomodulatory properties. *PLoS ONE*. 2013;8:e59354.
42. Apte MV, Pirola RC, Wilson JS. Pancreatic stellate cells: a starring role in normal and diseased pancreas. *Front Physiol*. 2012;3:344.
43. Wang J, Li T, Zhou Y, Wang X, Carvalho V, Ni C, et al. Genetic lineage tracing reveals stellate cells as contributors to myofibroblasts in pancreas and islet fibrosis. *iScience*. 2023;26:106988.
44. Jin G, Hong W, Guo Y, Bai Y, Chen B. Molecular mechanism of pancreatic stellate cells activation in chronic pancreatitis and pancreatic cancer. *J Cancer*. 2020;11:1505–15.
45. Asahina K, Tsai SY, Li P, Ishii M, Maxson RE Jr, Sucov HM, et al. Mesenchymal origin of hepatic stellate cells, submesothelial cells, and perivascular mesenchymal cells during mouse liver development. *Hepatology*. 2009;49:998–1011.
46. Zhou Y, Sun B, Li W, Zhou J, Gao F, Wang X, et al. Pancreatic stellate cells: a rising translational physiology star as a potential stem cell type for beta cell neogenesis. *Front Physiol*. 2019;10:218.
47. Xu W, Zhou Y, Wang T, Ni C, Wang C, Li R, et al. Mouse islet-derived stellate cells are similar to, but distinct from, mesenchymal stromal cells and influence the beta cell function. *Diabet Med*. 2024;41:e15279.
48. Ikejiri N. The vitamin A-storing cells in the human and rat pancreas. *Kurume Med J*. 1990;37:67–81.
49. Maden M. Retinoic acid in the development, regeneration and maintenance of the nervous system. *Nat Rev Neurosci*. 2007;8:755–65.
50. Chang H, Xiao X, Li M. The schizophrenia risk gene ZNF804A: clinical associations, biological mechanisms and neuronal functions. *Mol Psychiatry*. 2017;22:944–53.
51. FANTOM Consortium and the RIKEN PMI and CLST (DGT), Forrest ARR, Kawaji H, Rehli M, Baillie JK, de Hoon MJL, et al. A promoter-level mammalian expression atlas. *Nature*. 2014;507:462–70.
52. Mall R, Bynigeri RR, Karki R, Malireddi RKS, Sharma BR, Kanneganti T-D. Pancancer transcriptomic profiling identifies key PANoptosis markers as therapeutic targets for oncology. *NAR Cancer*. 2022;4:zcac033.
53. Song W, Liu Z, Wang K, Tan K, Zhao A, Li X, et al. Pyroptosis-related genes regulate proliferation and invasion of pancreatic cancer and serve as the prognostic signature for modeling patient survival. *Discov Oncol*. 2022;13:39.
54. Ediger BN, Du A, Liu J, Hunter CS, Walp ER, Schug J, et al. Islet-1 is essential for pancreatic  $\beta$ -cell function. *Diabetes*. 2014;63:4206–17.
55. Nekrep N, Wang J, Miyatsuka T, German MS. Signals from the neural crest regulate beta-cell mass in the pancreas. *Development*. 2008;135:2151–60.
56. Muñoz-Bravo JL, Hidalgo-Figueroa M, Pascual A, López-Barneo J, Leal-Cerro A, Cano DA. GDNF is required for neural colonization of the pancreas. *Development*. 2013;140:3669–79.

## Publisher's Note

Springer Nature remains neutral with regard to jurisdictional claims in published maps and institutional affiliations.